

Optimizing the delivery of deep brain stimulation using electrophysiological atlases and an inverse modeling approach

Kay Sun^a, Srivatsan Pallavaram^b, William Rodriguez^b, Pierre-Francois D'Haese^b, Benoit M. Dawant^b, Michael I. Miga^{*a}

^aDepartment of Biomedical Engineering, Vanderbilt University, Nashville TN 37235;

^bDepartment of Electrical Engineering and Computer Science, Vanderbilt University, Nashville TN 37235

* michael.miga@vanderbilt.edu; phone 1 615 343-8336; fax 1 615 343-7919

ABSTRACT

The use of deep brain stimulation (DBS) for the treatment of neurological movement degenerative disorders requires the precise placement of the stimulating electrode and the determination of optimal stimulation parameters that maximize symptom relief (e.g. tremor, rigidity, movement difficulties, etc.) while minimizing undesired physiological side-effects. This study demonstrates the feasibility of determining the ideal electrode placement and stimulation current amplitude by performing a patient-specific multivariate optimization using electrophysiological atlases and a bioelectric finite element model of the brain. Using one clinical case as a preliminary test, the optimization routine is able to find the most efficacious electrode location while avoiding the high side-effect regions. Future work involves optimization validation clinically and improvement to the accuracy of the model.

Keywords: Deep brain stimulation, finite element modeling, optimization

1. INTRODUCTION

Deep brain stimulation (DBS) is a potentially effective treatment for neurological movement degenerative disorders such as Parkinson's disease and Dystonia. The technique involves electrically stimulating critical structures of the brain believed to affect the involuntary movements using implanted electrodes. The treatment, however, is still in its developmental stages and its mechanism is still not fully understood. Currently, the procedure involves first inserting intraoperative electrodes in the brain using a stereotactic frame whose trajectories are determined based on general locations of the critical structures like subthalamic nucleus (STN) and internal global pallidus (GPi). The exact depth along the trajectory for implantation is unknown. As a result, these smaller intraoperative electrodes are stepped incrementally into brain and physiological response from the patient recorded to fine tune the precise position. Once a position with superior response is obtained, the intraoperative electrodes are removed and a permanent, larger stimulating electrode is implanted. When the patient is post-procedurally stable, stimulation parameters (amplitude, pulse width and frequency) are then explored to establish the best therapeutic response. This manual process of looking for the best electrode position and stimulation amplitude in the operating room may miss potentially more effective single and/or multi-electrode configurations as an exhaustive search is intraoperatively time prohibitive and the added time compromises the patient.

Previous studies have concentrated on determining the best electrode placement using anatomical locations as their guide [1,2]. However, these critical targeted anatomical structures are difficult to distinguish clearly on magnetic resonance (MR) or computed tomography (CT) images. Although atlas-based segmentation may help identify these structures, errors could stem from registration of patient images to these atlases, limited resolution of the patient images and even inaccuracies from the atlases themselves. An alternative approach to help identify electrode placement targets is with probabilistic electrophysiological maps that are based on physiology as opposed to anatomy. The maps are based on an extensive collection of intraoperative patient data and are nonrigidly registered to the patient-specific preoperative images to identify regions in the patient's brain likely to produce efficacy in the form of symptom relief and those likely to produce undesired side-effects [3,4]. The goal of this study is to perform a multivariate optimization for the intraoperative electrode selection, placement and stimulation amplitude using electrophysiological maps of the brain and

a computational bioelectric brain model. The bioelectric brain model predicts the shape and extent of the electric field generated by the electrodes that may invoke action potentials in nearby neurons. While a more complete treatment of this problem involves determining the distribution of the electric field along the neuron/axon complex, accounting for tissue-electrode interface and incorporation of patient-specific anatomical models, the aim of this preliminary work is to test the feasibility of optimizing the stimulation field itself in relation to the efficacy and side-effect maps. If possible, the next step would be to account for these additional model complexities, and test during intraoperative programming. Underlying this development is the hypothesis that an optimum electrode configuration determined intraoperatively will translate to improved postoperative therapeutic programming outcomes. In this initial work, the optimization routine was tested on 2 simulated condition sets and 1 clinical data set (patient-specific) electrophysiological maps.

2. METHODOLOGY

2.1 Bioelectric finite element model

A 3-dimensional finite element model of 5 intraoperative DBS electrodes inserted into brain tissue was created using COMSOL version 4.0a (COMSOL, Inc., Burlington, MA). To simulate the electric potential distribution resulting from stimulation, Poisson's equation for conductive media was used [5],

$$\nabla \cdot (\sigma \nabla V) = -I \quad (1)$$

where σ is the conductivity, V is the electric potential and I is the current source. In this preliminary work, the brain tissue geometry was represented as a cylinder consisting of approximately 80,300 tetrahedral elements and assumed to be homogeneous and isotropic with conductivity of 0.3 S/m [6]. Since the primary focus of this study is to optimize the electrode(s) placement and amplitude(s) of stimulation, capacitive effects were neglected and electrostatic conditions were assumed which allowed for tractable computation time using the multi-physics solver COMSOL linked with MATLAB (MathWorks, Inc., Natick, MA). The 5 DBS electrode configuration (FHC, Inc., Type D: Differential microTargeting Electrode) consists of a central electrode with the remaining 4 electrodes being placed a distance of 2 mm anterior, posterior, lateral, and medially, respectively. Each electrode is made up of a conducting contact, an insulating shaft and a larger grounded cannula (Figure 1). The size of the brain cylinder was set large enough so as to eliminate far-field boundary effects. Current sources were assigned to the 5 contacts and allowed to vary in magnitude. The entire electrode was also allowed to vary in position. Since the 5-electrode implant method is constrained to move along insertion tracks, variability in position is a one degree of freedom translation in the direction of depth. A full remeshing of the geometries occurred with each adjustment in electrode depth.

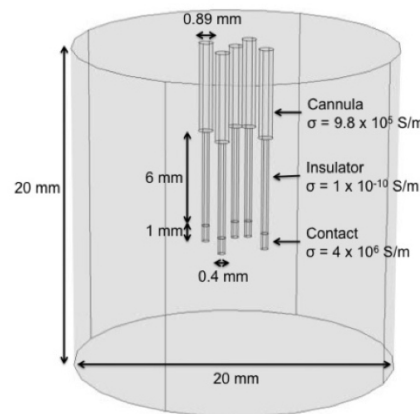


Figure 1. Model of the 5 intra-operative DBS electrodes within the cylindrical brain tissue geometry. The conducting contacts are at the tips and separated from the thicker grounded cannula by the insulating shaft in between.

2.2 Optimization

In this investigation, desired stimulation efficacy zones from efficacy map (E) and undesired side-effect zones from side-effect map (S) are physiologically triggered when the brain tissue potential at those locations becomes elevated above a certain tissue activation voltage (TAV) level (TAV = -0.7 V [7]). It must be stressed that this assumption of a TAV is a gross oversimplification of the complex relationship between voltage and neuron activation. In addition to the electric potential, neural response is dependent on the size, location and orientation of the neurons, which have wide ranges in values and are highly patient-specific. Although accurately predicting the shape and volume of neural tissue activation is important, the emphasis of this study is in demonstrating the feasibility of developing an optimization framework for determining the ideal electrode selection, placement and stimulation amplitude based on the patient-specific electrophysiological atlas.

The goal of the optimization is to position and power the 5 electrodes such that the electric potential distribution produced is sufficient to activate high-efficacy zones for therapeutic benefit while avoiding activation of the side-effect zones. Towards this goal, the objective function, G , for minimization was written as,

$$\min \{G(A_i \{depth, amplitude\})\} = 1 - \frac{\sum_{i=1}^N E'_i A_i}{1 + \sum_{i=1}^N (1 - E'_i) A_i} + \frac{\sum_{i=1}^N S'_i A_i}{1 + \sum_{i=1}^N A_i} \quad (2)$$

where E'_i and S'_i are the normalized efficacy and side-effect map values for the i th voxel (values range from 0 to 1 with values of unity indicating high efficacy or high side-effect, respectively) and are interpolated to 3D image volume grid associated with the patient. Normalization by the maximum value in each map was required to equalize the weighing factors from both maps. A_i represents the i th voxel of a binary mask of the tissue activated volume determined by the electric potential solved by COMSOL. Specifically, with each candidate depth and electrode amplitude, COMSOL is invoked to calculate the potential field, which is then interpolated onto the same 3D image volume as the probabilistic maps. The electric potentials at the i th voxel over N voxels are used to generate a binary mask whereby all regions above the TAV are assigned unity. The general construction of the objective function in Eq. 2 is to select configurations that attempt to improve the ratio of activated efficacious regions over those that are not efficacious while simultaneously penalizing configurations that improve the ratio of activated side-effect regions over the activated regions. The first term, the constant 1, is present to offset the objective function when no brain tissue is activated. The second term balances the brain tissue activation in the more desired over less desired zones so that there is no unnecessary tissue activation in lesser efficacy zones that are important when considering power constraints for the DBS power supply. These two terms serve to produce the optimum for only the efficacy map. The side-effect map is taken into account by the third term, which adjusts for when the undesired zones are activated.

The global minimization function “patternsearch” in MATLAB was used for the multivariable optimum search. It has the potential to avoid local minima by being a set-based method rather than gradient-based. Briefly, a set of points for evaluation is first determined and their objective functions calculated and polled to find their minimum. If a minimum is found, then polling is successful and the domain for the next set of points is decreased. Otherwise, the domain is increased to expand the search area. The process is repeated until the convergence tolerance to the objective function is reached. The initial guess for electrode depths was set at the center of the maps, which were defined at depth 0 mm, and at half maximum amplitude (-7.9 mA) for all electrodes. The optimization was constrained with lower and upper bounds for electrode depth at -5 and +5 mm, respectively from the initial implant depth. Their stimulation amplitudes were constrained from -15.9 to 0 mA. The overall optimization routine is outlined in Figure 2.

In addition to a patient-specific electrophysiological atlas, simulated efficacy and side-effect maps were generated to further evaluate and validate the objective function in Eq. 2. These maps were created using the electric potential distributions from the electrodes in the bioelectric brain model to duplicate high and low efficacy and side-effect values. The locations of these values were strategically selected to lie between the electrode trajectory paths in the actual optimization in order to test more extreme scenarios where multiple electrodes may be optimal.

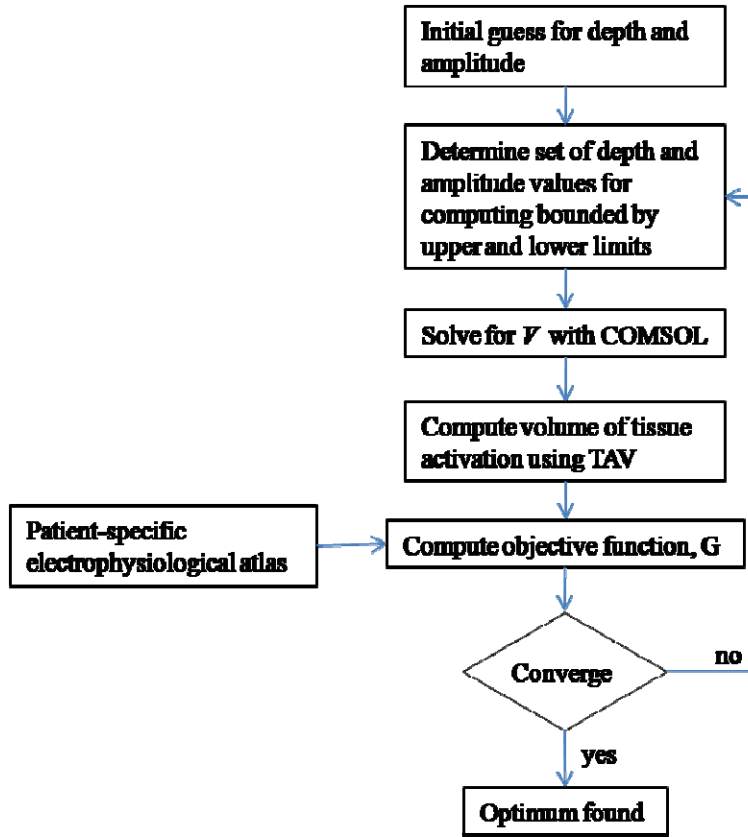


Figure 2. A flowchart summarizing the optimization routine.

3. RESULTS

The first set of simulated electrophysiological maps has high efficacy (colored in red) and low side-effect (colored in blue) regions centered at the same position, at -1 mm in lateral direction and -1 mm in depth (Figure 3a and b). All other regions have high side-effect values (colored in red). This scenario was designed to have just one optimum solution that is from the voltage overlap from 2 adjacent electrodes along X = 0 mm and X = -2 mm trajectory path, and no electrode along the X = +2 mm path. The objective function was able to successfully locate those exact 2 electrodes, and optimized their depth and stimulation current amplitude for best overlap with the simulated maps (Figure 4).

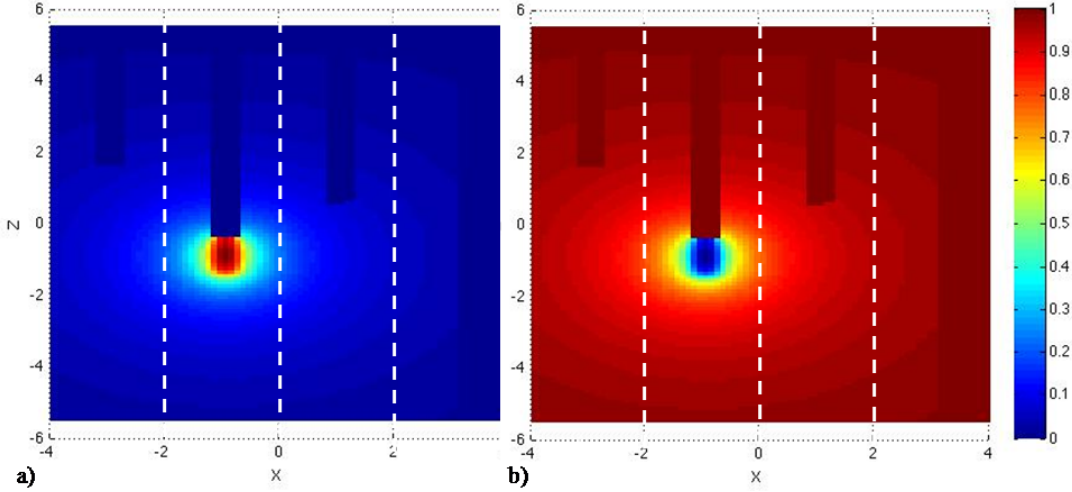


Figure 3. The first test of the objective function using simulated (a) efficacy and (b) side-effect maps. Unity represented by red in the colorbar is high probability for efficacy in the efficacy map and high probability for side-effect in the side-effect map. Low probability for efficacy and side-effect is indicated by blue in the colorbar. The dashed lines are the electrode trajectory paths for the optimum routine.

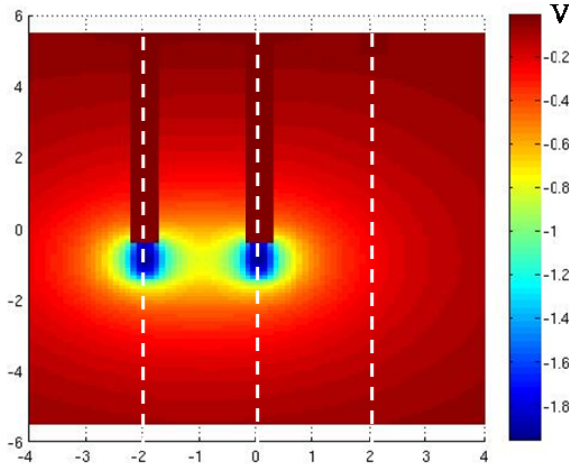


Figure 4. The electric potential distribution of the optimized electrode position and stimulation current amplitude for the first simulated test. Note the voltages are negative values since the contacts are set as cathodes. For this colorbar, red represent zero voltage while blue represent high negative voltage. The dashed lines are the electrode trajectory paths for the optimum routine.

The second simulated map set tested the relationship between efficacy and side-effect components in the objective function. For the efficacy map, there are 3 high efficacy regions (colored in red) all at depth -1 mm. Observing the efficacy map solely, the optimum would result in the simultaneous stimulation of the 3 electrodes at $X = 0, -2$ and $+2$ mm trajectory paths, all at depth -1 mm (Figure 5a). However, the side-effect map prescribed an additional constraint such that there is just one region where side-effect value is the lowest (colored in blue in Figure 5b). So the optimum for this test is 2 electrodes at $X = 0$ mm and -2 mm paths. The objective function proposed in Eq. 2 was once again successful in this test, selecting those exact 2 electrodes, and optimized their depth and stimulation current amplitude for optimum voltage overlap (Figure 6). Note, the optimization found a higher optimum current amplitude for the electrode at $X = 0$ mm than the electrode at $X = -2$ mm despite the more intuitive optimum of the same current amplitude for both

electrodes. The reason for the lower objective function for different current amplitudes than for the same amplitude values is that the penalty due to the activation volume overlap with the side-effect map from one high value amplitude electrode is lower than the combined penalties from the overlap with side-effect map from two middle value amplitude electrodes.

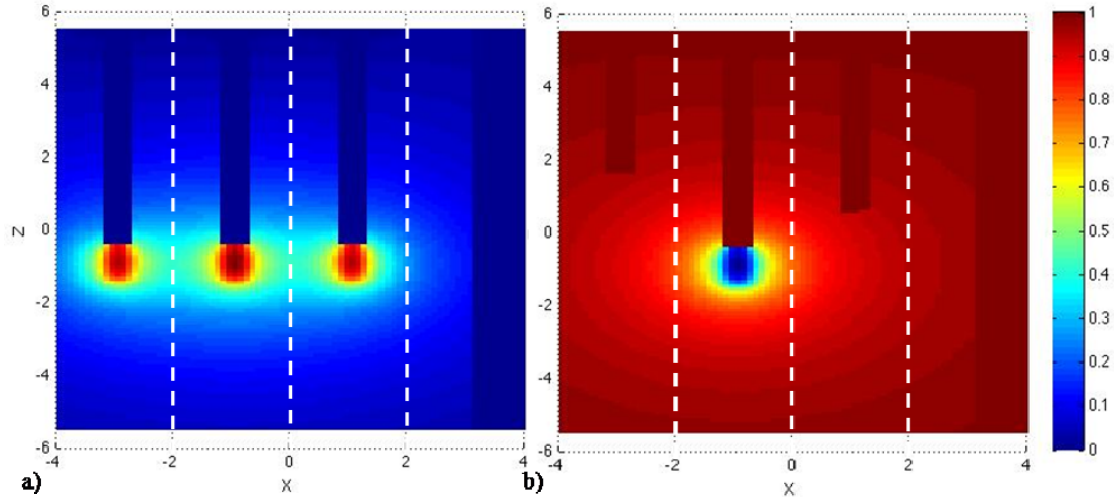


Figure 5. The second test of the objective function using simulated (a) efficacy and (b) side-effect. Unity represented by red in the colorbar is high probability for efficacy in the efficacy map and high probability for side-effect in the side-effect map. Low probability for efficacy and side-effect is indicated by blue in the colorbar. The dashed lines are the electrode trajectory paths for the optimum routine.

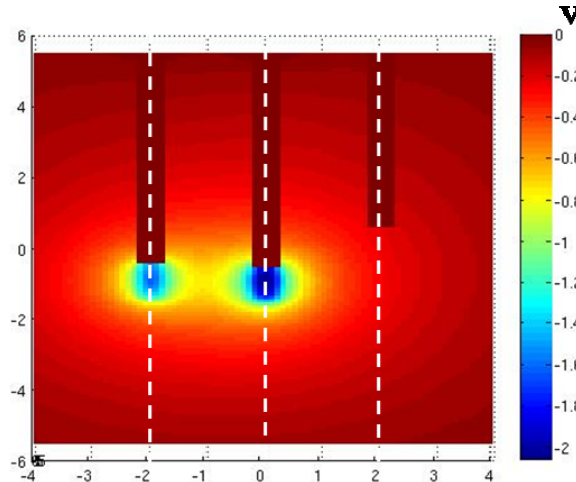


Figure 6. The electric potential distribution of the optimized electrode position and stimulation current amplitude for the second simulated test. Note the voltages are negative values since the contacts are set as cathodes. For this colorbar, red represents zero voltage while blue represents high negative voltage. The dashed lines are the electrode trajectory paths for the optimum routine.

For the clinical case, the optimum depth and current amplitude for the 5 electrodes are tabulated in Table 1. No power was needed for the center, anterior, posterior and lateral electrodes. Only medial electrode was needed. Figure 7 shows the optimized brain tissue activation regions (based on the optimum configuration in Table 1) overlaid with efficacy and side-effect maps of a candidate patient. Despite having no single electrode trajectory path that passes through the heart of the efficacy region (circled in Figure 7a), the optimization routine is able to find the next most efficacious location (in red) while avoiding the high side-effect regions (in red to yellow).

Table 1. Optimum depth and amplitude for the 5 intraoperative electrodes.

	Depth [mm]	Amplitude [mA]
Center	5.00	0.0
Anterior	5.00	0.0
Posterior	2.50	0.0
Lateral	-0.31	0.0
Medial	3.59	-2.0

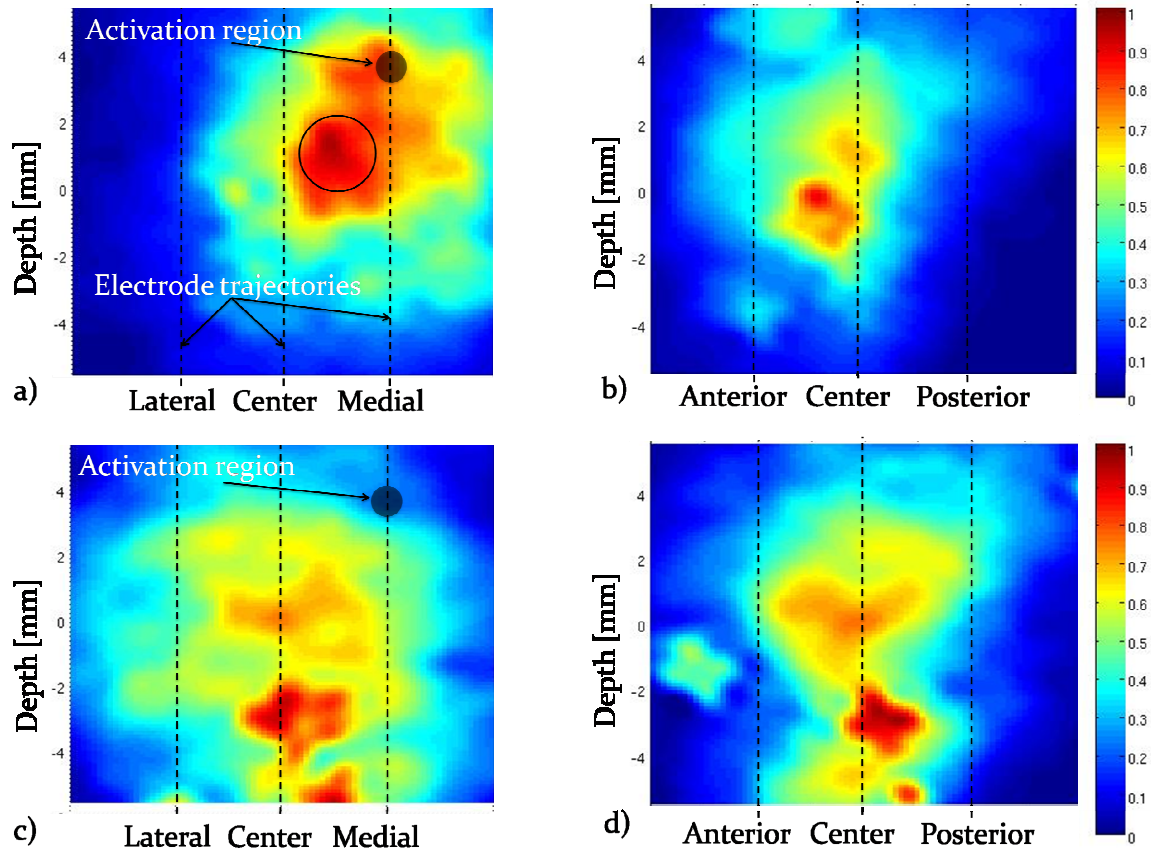


Figure 7. Cross-sectional views of the optimized brain tissue activation region (in grey) overlaid with the (a-b) efficacy and (c-d) side-effect map (colored). Unity is at the highest efficacy or side-effect. Dashed lines represent the electrode trajectories.

4. CONCLUSIONS

There has been considerable research in the simulation of DBS via finite elements methods [5, 8,9,10], but no work to our knowledge has involved the optimization of the surgical procedure itself via a coupled inverse modeling with probabilistic map framework as performed here. While aspects are somewhat idealized here, the results suggest that computational multivariate optimization of electrode selection, placement and amplitude in DBS based on electrophysiological atlases is feasible and can be easily calculated as part of the trajectory planning steps. Ultimately, this additional information may provide the best patient-specific electrode configuration for use during preoperative planning, intraoperative navigation and postoperative programming phases. The bioelectric brain model used here is limited in its simplicity, but future work will involve improving the accuracy of the models with more realistic tissue

properties, simulating more realistic stimulation settings with time dependent analysis and incorporating neuron modeling to get a more accurate tissue activation volume. Lastly, further testing of the objective function and validation with clinical observations will have to be performed too. Nevertheless, this preliminary study offers an exciting new optimization framework within the field of DBS therapeutic delivery.

ACKNOWLEDGEMENTS

This work was supported by the National Institute of Health - National Institute of Biomedical Imaging and Bioengineering under grant award # R01 EB006136.

REFERENCES

- [1] Butson, C., Cooper, S., Henderson, J., Wolgamuth, B. and McIntyre, C., "Probabilistic analysis of activation volumes generated during deep brain stimulation," *NeuroImage* 54, 2096-2104 (2011).
- [2] Butson, C., Cooper, S., Henderson, J. and McIntyre, C., "Patient-specific analysis of the volume of tissue activated during deep brain stimulation," *NeuroImage* 34, 661-670 (2007).
- [3] Pallavaram, S., D'Haese, P. F., Kao, C., Yu, H., Remple, M., Neimat, J., Konrad, P. and Dawant, B., "A new method for creating electrophysiological maps for DBS surgery and their application to surgical guidance," *Med Image Comput Comput Assist Interv* 11(Pt 1), 670-677 (2008).
- [4] D'Haese, P. F., Pallavaram, S., Li, R., Remple, M., Kao, C., Neimat, J., Konrad, P., and Dawant, B., "CranialVault and its Crave tools: A clinical computer assistance system for DBS therapy," *Med Image Anal* 1, (2010).
- [5] Butson, C. and McIntyre, C., "Tissue and electrode capacitance reduce neural activation volumes during deep brain stimulation," *Clin Neurophysi* 116, 2490-2500 (2005).
- [6] Rank Jr, J., "Specific impedance of rabbit cerebral cortex," *Exp Neurol* 7, 144-152 (1963).
- [7] Kao, C. and Coulter, D., "Physiology and pharmacology of corticothalamic stimulation-evoked responses in rat somatosensory thalamic neurons in vitro," *J Neurophysiol* 77, 2661-2676 (1977).
- [8] Butson, C. and McIntyre, C., "Current steering to control the volume of tissue activated during DBS," *Brain Stimul* 1(1), 7-15 (2008).
- [9] Aström, M., Zrinzo, L., Tisch, S., Tripoliti, E., Hariz, M. and Wårdell, K., "Method for patient-specific finite element modeling and simulation of DBS," *Med Biol Eng Comput* 47(1), 21-28 (2009).
- [10] Chaturvedi, A., Butson, C., Lempka, S., Cooper, S. and McIntyre, C., "Patient-specific models of deep brain stimulation: Influence of field model complexity on neural activation predictions," *Brain Stimul* 3, 65-77 (2010).